MicroRNA-351 promotes schistosomiasis-induced hepatic fibrosis by targeting the vitamin D receptor

Xing He[a,1], Yue Sun[a,b,1], Nanhang Lei[a], Xiaobin Fan[a], Cheng Zhang[a], Yange Wang[a], Kuiyang Zheng[b], Dongmei Zhang[a,2], and Weiqing Pan[a,2]

[a]Department of Tropical Infectious Diseases, Second Military Medical University, Shanghai 200433, China; and [b]Department of Pathogen Biology and Immunity, Xuzhou Medical University, Xuzhou 221000, China

Edited by Thomas E. Wellems, National Institutes of Health, Bethesda, MD, and approved November 29, 2017 (received for review September 18, 2017)

Aberrant expression of microRNAs (miRNAs) underlies a spectrum of human diseases including organ fibrosis, and hepatic stellate cells (HSCs) are the main effectors of hepatic fibrosis. Here, we showed that the expression of host *miR-351* in HSCs was markedly reduced during the early stage of *Schistosoma* infection. However, this expression was significantly increased during the later stage of infection (after 52 d of infection). The elevated levels of *miR-351* promoted hepatic fibrosis by targeting the vitamin D receptor (VDR), which is an antagonist of SMAD signaling. Importantly, efficient and sustained inhibition of *miR-351* in liver tissues using the highly hepatotropic recombinant adeno-associated virus serotype 8 (rAAV8), alleviated the hepatic fibrosis, partially protecting the host from lethal schistosomiasis. In addition, we found that *miR-351* is negatively regulated by IFN-γ in HSCs during infection. At the early stage of infection, the elevated levels of IFN-γ inhibited the expression of *miR-351* in HSCs through activation of signal transducer and activator of transcription 1 and induction of IFN regulatory factor 2, which binds the promotor of *pre–miR-351*. Our study provides insights into the mechanisms by which *miR-351* regulates schistosomiasis hepatic fibrosis and highlights the potential of rAAV8-mediated *miR-351* inhibition as a therapeutic intervention for fibrotic diseases.

microRNA | schistosomiasis | hepatic fibrosis | vitamin D receptor | gene therapy

Schistosomiasis is caused by several species of trematode worms. It affects more than 230 million people worldwide, resulting in around 70 million disability-adjusted life years lost annually (1, 2). The pathology resulting from infection with the helminth parasites *Schistosoma mansoni* (*S. mansoni*) and *Schistosoma japonicum* (*S. japonicum*) is predominantly caused by the host reaction to parasite eggs, which are laid in the portal venous system and are subsequently trapped in the liver and intestine (3, 4). The egg-induced hepatic fibrosis, which can lead to portal hypertension, is the primary cause of morbidity and mortality associated with this chronic disease (1). Elucidating the mechanisms that result in hepatic fibrosis may lead to more effective strategies for intervention for schistosomiasis and a variety of fibrotic diseases.

Hepatic stellate cells (HSCs) are the main effectors for various types of hepatic fibrosis (5), including the hepatic fibrosis induced by schistosome infection (6). When liver injury occurs, quiescent HSCs, characterized by the presence of cytoplasmic vitamin A droplets, are activated to become proliferative, contractile, and fibrogenic myofibroblasts. HSCs secrete excess extracellular matrix (ECM) in the liver, resulting in fibrosis (7). Transforming growth factor 1 (TGF-β1), derived from paracrine and autocrine sources, remains the classic fibrogenic cytokine driving the activation of HSCs. Signals downstream of TGF-β1 depend on SMAD proteins, in which SMAD2 and -3 are stimulatory and SMAD7 is inhibitory (8). Vitamin D receptor (VDR) is an antagonist of SMAD signaling, which inhibits the residency of SMAD on chromatin to suppress SMAD-dependent gene expression (9). Blocking the activation of HSCs has become one of the major strategies for therapeutic interventions for hepatic fibrosis (10).

Dysregulation of miRNA expression is involved in a spectrum of human diseases, including organ fibrosis (11, 12). Our previous data indicated that *miR-21* was up-regulated in HSCs following infection with *S. japonicum*, and this induced hepatic fibrogenic effects by targeting SMAD7, an antagonist of SMAD signaling (13). Up-regulation of *miR-351* expression was detected by miRNA assays in both schistosomiasis hepatic fibrosis and bleomycin-induced lung fibrosis (13, 14). Moreover, we found that VDR is a predicted target of *miR-351*. In this study, we demonstrated that host *miR-351* promotes the progression of schistosomiasis-related hepatic fibrosis by targeting VDR, and inhibition of *miR-351* mediated by recombinant adeno-associated virus 8 (rAAV8) in the liver protected mice from lethal infection by alleviating hepatic fibrosis in a well-studied model of human schistosomiasis. Furthermore, we revealed the molecular mechanism underpinning the regulation of *miR-351* following infection.

Results

Protection of Mice Against Lethal *Schistosoma* Infection by Inhibition of *miR-351* Through Attenuation of Hepatic Fibrosis. Our previous study identified a number of host miRNAs by expression profiling that were up-regulated during the progression of hepatic fibrosis associated with schistosomiasis. This included *miR-351* (13). We verified the up-regulation of *miR-351* in the infected livers of mice (*SI Appendix*, Fig. S1*A*). Because of the key roles of

Significance

Hepatic fibrosis is the final common pathological outcome of many chronic liver diseases and occurs when hepatic stellate cells (HSCs) are activated to become fibrogenic myofibroblasts. To date, there are still no approved antifibrotic therapies. Accumulating evidence suggests that targeting the deregulated miRNAs could mitigate disease outcomes. In this study, using a well-studied model of human schistosomiasis, we show that elevated *miR-351* promotes the activation of HSCs after infection by targeting the vitamin D receptor, and inhibition of *miR-351* in the liver mediated by rAAV8 protects the host from lethal infection by alleviating hepatic fibrosis. This study provides insights into the mechanisms that result in schistosomiasis-related hepatic fibrosis and targets of intervention for schistosomiasis and other fibrotic diseases.

Author contributions: X.H., D.Z., and W.P. designed research; X.H., Y.S., N.L., X.F., C.Z., and Y.W. performed research; X.H. contributed new reagents/analytic tools; X.H., Y.S., K.Z., D.Z., and W.P. analyzed data; and X.H. and W.P. wrote the paper.

The authors declare no conflict of interest.

This article is a PNAS Direct Submission.

[1]X.H. and Y.S. contributed equally to this work.

[2]To whom correspondence may be addressed. Email: dmzhangcn@163.com or wqpan0912@aliyun.com.

This article contains supporting information online at www.pnas.org/lookup/suppl/doi:10.1073/pnas.1715965115/-/DCSupplemental.

HSCs in the development of hepatic fibrosis, we quantified the expression of *miR-351* in the HSCs from *S. japonicum*-infected livers. We found that the abundance of *miR-351* in HSCs was significantly higher than that in the hepatocytes ($P < 0.001$) and Kupffer cells ($P < 0.001$) (*SI Appendix*, Fig. S1*B*). In addition, the fold change of miR-351 expression alteration after infection in HSCs was also significantly higher than that in the hepatocytes ($P < 0.001$) and Kupffer cells ($P < 0.001$) (*SI Appendix*, Fig. S1*C*).

To examine the role of *miR-351* in schistosomiasis-related hepatic fibrosis in vivo, mice were first infected with a lethal dose of *S. japonicum* cercariae. Next, they were i.v. injected with a rAAV8–*miR-351*–sponge vector for sustained *miR-351* inhibition, a control vector, or PBS at day 10 postinfection. We found that a single dose of rAAV8–*miR-351*–sponge partially protected infected mice from the lethal effects of schistosomiasis, and 8/10 of these mice survived until the end of the 80-d study (Fig. 1*A*). In contrast, all mice receiving the control vector ($n = 10$) or PBS ($n = 10$) died within 9 wk of infection (Fig. 1*A*).

Hepatic fibrosis is the primary cause of death for hosts infected with schistosome (1), so we next investigated whether the rAAV8–*miR-351*–sponge-mediated protection involved attenuation of hepatic fibrosis. Mice were exposed to a mild dose of parasites and then treated with the vectors or PBS. This revealed that, by 8 wk of infection, mice receiving rAAV8–*miR-351*–sponge displayed a significant reduction in ECM deposits, as shown by hydroxyproline quantification (Fig. 1*B*) and Masson's trichrome staining (Fig. 1 *C* and *E*), in addition to a marked reduction in the size of hepatic granulomas visualized by H&E staining (Fig. 1 *D* and *E*). This reduction was confirmed by qPCR and Western blot-based quantifications of fibrosis-associated gene expression in the livers of infected mice. The levels of *Col1α1*, *Col3α1*, and *α-SMA* were dramatically reduced in livers of mice treated with rAAV8–*miR-351*–sponge (Fig. 1 *F* and *G*). Hepatic fibrosis induced by schistosome infection is an immunological disease, and IL-13 and TGF-β1 play a crucial role in its progression through the SMAD pathway (13, 15). However, mRNA levels of *IL-13* and *TGF-β1* were similar in all groups of infected mice (Fig. 1*H*), indicating the regulation of the hepatic fibrosis by *miR-351* is independent of IL-13 and TGF-β1 production. Consistent with our previous study, the viral vector did not affect the survival or egg production of parasites in the hosts (*SI Appendix*, Fig. S2).

HSCs are the main effectors for hepatic fibrosis induced by schistosome infections. To investigate whether miR-351 can directly regulate the activity of HSCs, mice were exposed to a mild dose of parasites and then administered with vectors, and after 52 d of infection, primary HSCs were isolated to quantify the expression levels of HSC activation-associated genes, including *Col1α1*, *Col3α1*, and *α-SMA*. Our data showed that significantly increased collagen and *α-SMA* expression were observed in the infected mice without rAAV8–*miR-351*–sponge treatment compared with uninfected mice, while collagen and *α-SMA* expression were distinctly reduced in HSCs after the administration of rAAV8–*miR-351*–sponge (*SI Appendix*, Fig. S3), suggesting that miR-351 could promote the activation of HSCs in vivo.

Therapeutic Effect of Inhibition of miR-351 on Schistosomiasis-Related Hepatic Fibrosis. To investigate whether inhibition of *miR-351* in the liver can reverse hepatic fibrosis, mice were infected with a mild dose of parasites. At 42 d of infection, when hepatic fibrosis was clearly manifest, mice were treated with praziquantel to kill the parasite and then injected with either the

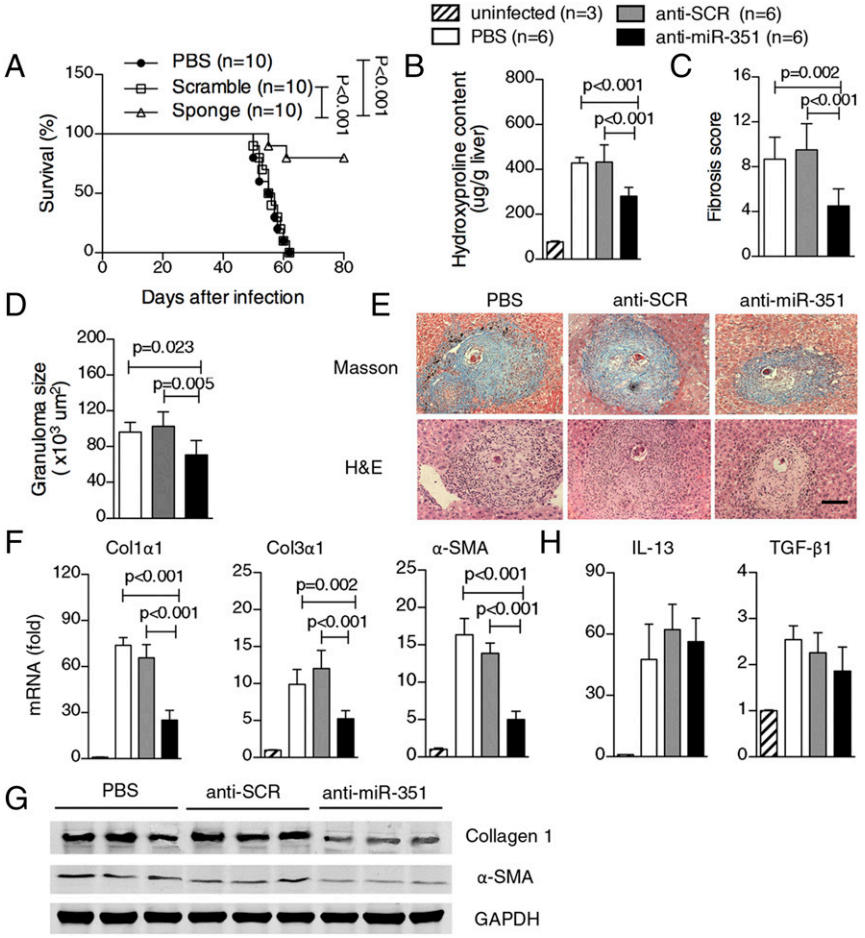

Fig. 1. Down-regulation of *miR-351* partially protects mice from lethal schistosome infections by attenuating hepatic fibrosis. (*A*) Mice were infected percutaneously with 30 *S. japonicum* cercariae at day 0 and treated with rAAV8–*miR-351*–sponge ($n = 10$) or control rAAV8 vectors ($n = 10$) at a dose of 1×10^{12} virus genomes or PBS ($n = 10$) by tail vein injection at day 10 postinfection. The animals were subjected to an 80-d survival study. Data are representative of three independent experiments. (*B–H*) Mice were infected percutaneously with 16 *S. japonicum* cercariae at day 0 or remained uninfected. Infected mice received rAAV8–*miR-351*–sponge or control rAAV8 vectors at a dose of 1×10^{12} virus genomes or PBS by tail injection at day 10 postinfection. Liver samples were collected at day 56 postinfection. Striped bars, uninfected mice ($n = 3$); white bars, mice receiving PBS ($n = 6$); gray bars, mice receiving rAAV8–scramble (SCR)–sponge ($n = 6$); black bars, mice receiving rAAV8–*miR-351*–sponge ($n = 6$). Hydroxyproline content in the liver (*B*). Fibrosis scores measured from Masson's trichrome staining of liver sections (*C*). Granuloma size measured from H&E staining of liver sections (*D*). Masson's trichrome staining and H&E staining of liver sections (*E*). (Scale bar, 200 μm.) qPCR analysis of levels of *Col1α1*, *Col3α1*, and *α-SMA* mRNA in the liver tissues (*F*). Parts of samples were selected for Western blot analysis of levels of collagen 1 and *α-SMA* in liver tissues (*G*). qPCR analysis of levels of *IL-13* and *TGF-β1* mRNA in liver tissues (*H*). Data are expressed as the mean ± SD of two independent experiments.

rAAV8 vectors or PBS. All of the mice were necropsied at 70 d of infection to evaluate hepatic fibrosis. As expected, hydroxyproline quantification and Masson's trichrome staining revealed that fibrosis in rAAV8–*miR-351*–sponge-treated mice was markedly reduced compared with that in the controls (*SI Appendix*, Fig. S4 *A*, *B*, and *D*). H&E staining indicated that the size of hepatic granulomas in the rAAV8–*miR-351*–sponge-treated group was also significantly smaller compared with controls (*SI Appendix*, Fig. S4 *C* and *D*). Western blot and qPCR confirmed the reduction in expression of *Col1α1*, *Col3α1*, and *α-SMA* (*SI Appendix*, Fig. S4 *E* and *F*). Likewise, mRNA levels of *IL-13* and *TGF-β1* were similar in all groups of infected mice (*SI Appendix*, Fig. S4*G*), and the livers showed no significant changes in egg burden (*SI Appendix*, Fig. S4*H*).

MiR-351 Regulates Hepatic Fibrosis by Targeting VDR in HSCs. We performed a computational analysis using the TargetScan database to search for putative targets of *miR-351*. We found that VDR, an antagonist of HSC activation (9), is a predicted target of *miR-351* (Fig. 2*A* and *SI Appendix*, Fig. S5). To validate the relationship between *miR-351* and VDR, we first analyzed their expression in HSCs during infection. Unlike its expression in whole livers (*SI Appendix*, Fig. S1*A*), *miR-351* in the HSCs was decreased at days 32 and 42 postinfection, and then significantly increased by day 52 postinfection (Fig. 2*B*). Meanwhile, the expression of VDR showed the opposite trend: it was elevated at days 21 and 32 postinfection, and then significantly lower at day 42, and the lowest levels were observed at day 52 postinfection (Fig. 2*C*). To validate VDR as a *miR-351* target, we generated a reporter construct that contains the firefly luciferase gene fused to the 3′ UTR of *VDR*, which contained a putative *miR-351* target site (Fig. 2*A*). This construct was transiently transfected into 293T cells together with either *miR-351* mimics or a negative control miRNA. We observed a strong reduction in luciferase activity in cells transfected with both the *miR-351* mimics and the VDR–UTR plasmids (Fig. 2*D*). In contrast, mutation of five nucleotides in the *miR-351* target sequence led to a complete abrogation of reporter inhibition (Fig. 2*D*). Furthermore, we transfected either *miR-351* mimics or inhibitors into primary HSCs from uninfected mice and quantified the level of VDR by qPCR and Western blot. Our data revealed that at both the mRNA and protein levels, elevation of *miR-351* significantly reduced the expression of VDR, while depletion of *miR-351* significantly increased the expression (Fig. 2 *E* and *F*). Finally, we analyzed *VDR* levels in the liver tissues and primary HSCs from infected livers treated with rAAV8–*miR-351*–sponge at week 8 postinfection and found that *VDR* expression was markedly increased as a result of reduction of *miR-351* (Fig. 2 *G*–*I*). Taken together, these data indicate that *VDR* is a direct target of *miR-351* in HSCs.

IFN-γ Inhibits the Expression of miR-351 in HSCs by Induction of IFN Regulatory Factor 2. We next investigated the molecular mechanisms by which schistosome infection regulates the expression of *miR-351*. It is well documented that during the early stages of schistosome infection, IFN-γ expression is induced, while at the later stages when liver-trapped eggs are present, its expression declines (3). We found the IFN-γ expression dynamics in the liver tissues were negatively correlated with the kinetics of *miR-351* in isolated HSCs from the corresponding diseased livers during infection (*SI Appendix*, Fig. S6). This prompted us to ask whether IFN-γ regulates *miR-351* expression in HSCs. To test this, we stimulated primary HSCs isolated from uninfected mice with recombinant IFN-γ. The IFN-γ significantly reduced *miR-351* expression, but not *miR-21* (Fig. 3*A*). This inhibition was dependent on signal transducer and activator of transcription 1 (STAT1), a pivotal molecule in IFN-γ signal transduction (16). This is because knocking down *STAT1* using siRNAs significantly elevated expression of *miR-351* (Fig. 3*B* and *SI Appendix*, Fig. S7). Next, we investigated how IFN-γ regulates *miR-351* expression. We examined the putative promoter extending 2,000 bp upstream of the coding region of *pre–miR-351* and identified one highly conserved putative binding site for IFN regulatory factor 2 (IRF2) (Fig. 3*C*), a transcriptional repressor in the IFN-γ–mediated pathway (17). We found that IFN-γ

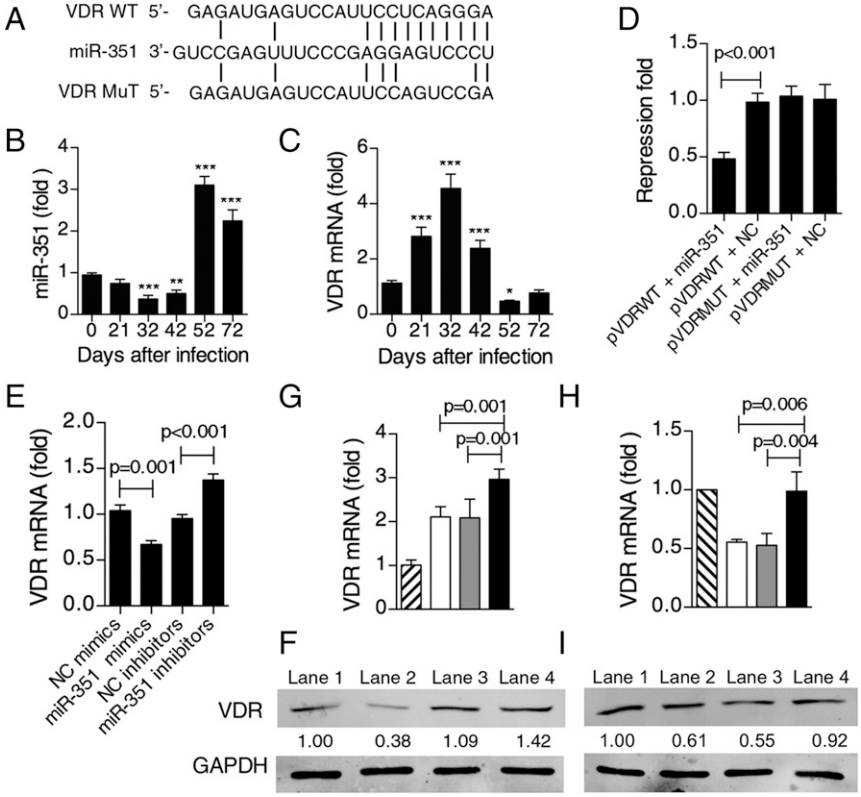

Fig. 2. Validation of the relationship between miR-351 and VDR. (*A*) Sequence alignment of *miR-351* and its target sites in the 3′ UTR of *VDR*. (*B* and *C*) Expression of *miR-351* (*B*) and *VDR* mRNA (*C*) in primary HSCs during infection was detected by qPCR ($n = 4$). $^*P < 0.05$, $^{**}P < 0.001$, $^{***}P < 0.001$, compared with samples from day 0. (*D*) Luciferase reporter assays for 293T cells transfected with pRL-TK vectors carrying VDR wild type (WT) 3′ UTR, or VDR mutant (Mut) 3′ UTR in the absence or presence of *miR-351* mimics ($n = 3$). (*E* and *F*) Expression of VDR in primary HSCs transfected with *miR-351* mimics or inhibitors was detected by qPCR ($n = 3$) (*E*) and Western blot (*F*). Lanes are as follows: 1, negative control (NC) mimics; 2, miR-351 mimics; 3, NC inhibitors; and 4, *miR-351* inhibitors. (*G*) The expression of VDR mRNA in the liver tissues from mice at week 8 postinfection after the administration of rAAV8 vectors. Striped bars, uninfected mice ($n = 3$); white bars, mice receiving PBS ($n = 6$); gray bars, mice receiving rAAV8–scramble (SCR)–sponge ($n = 6$); and black bars, mice receiving rAAV8–*miR-351*–sponge ($n = 6$). (*H* and *I*) The expression of VDR in primary HSCs from mice at week 8 postinfection was detected by qPCR (*H*) and Western blot (*I*) after the administration of rAAV8 vectors. Striped bars, uninfected mice; white bars, mice receiving PBS ($n = 3$); gray bars, mice receiving rAAV8–scramble (SCR)–sponge ($n = 3$); and black bars, mice receiving rAAV8–*miR-351*–sponge ($n = 4$). Lanes are as follows: 1, uninfected; 2, PBS; 3, anti-SCR; and 4, *anti–miR-351*. Data are expressed as the mean ± SD of three independent experiments.

stimulation significantly increased IRF2 expression. This was accompanied by the phosphorylation of STAT1, which inhibited *miR-351* in a time-dependent manner (Fig. 3 *D* and *E*). Both phosphorylation of STAT1 and expression of IRF2 in HSCs increased during the early phases of schistosome infection and then decreased during the later stages (Fig. 3*F*), suggesting an inverse relationship with the expression of *miR-351* (Fig. 2*B*). Furthermore, knocking down *IRF2* expression using siRNAs completely abrogated the inhibitory effect of IFN-γ on *miR-351* expression (Fig. 3*G* and *SI Appendix*, Fig. S7).

To validate the activity of this putative binding site, we generated a construct expressing luciferase under its control. IFN-γ significantly attenuated the expression of the luciferase reporter gene in 293T cells (Fig. 3*H*). In addition, chromatin immunoprecipitation (ChIP) analysis further validated the activity of this putative binding site. Our results showed that IRF2 can be recruited to the *pre–miR-351* promotor in HSCs after IFN-γ stimulation in vitro (Fig. 3*I*) or after infection (day 32 postinfection) in vivo (Fig. 3*J*). Collectively, these data reveal that IFN-γ inhibits the expression of *miR-351* in HSCs through induction of *IRF2*, which binds the promotor of *pre–miR-351*.

IFN-γ Blocks Activation of HSCs Through miR-351–Mediated Up-Regulation of VDR. It is well known that HSCs contribute to hepatic fibrosis. Several studies reported that IFN-γ blocks the activation of HSCs through the induction of SMAD7, an antagonist of TGF-β/SMAD signaling (18, 19). This interferes with the activation of SMAD2 and SMAD3 by preventing their receptor interaction and phosphorylation (20). We observed a similar phenotype using IFN-γ to stimulate primary HSCs in vitro. After IFN-γ stimulation, the expression of *Col1α1* and *α-SMA* (two markers of HSC activation) was strongly suppressed, while SMAD7 was induced (*SI Appendix*, Fig. S8*A*). In addition to SMAD7, our data also indicated that IFN-γ significantly induced the expression of VDR (*SI Appendix*, Fig. S8*A*), an antagonist of TGF-β/SMAD signaling (9). VDR antagonizes SMAD residency on chromatin to suppress SMAD-dependent gene expression (9). Because our data showed that IFN-γ inhibits the expression of *miR-351*, and VDR is a direct target of *miR-351* in HSCs, we speculated that IFN-γ blocks the activation of HSCs via increasing expression of VDR as a result of inhibition of *miR-351*. To address this, we transfected *miR-351* inhibitors into primary HSCs. This showed that *miR-351* knockdown partially recapitulated the effect of IFN-γ–mediated inhibition on HSC activation by induction of VDR instead of SMAD7 (*SI Appendix*, Fig. S8*B*). Furthermore, knockdown of VDR or SMAD7 only partially weakened the effect of IFN-γ–mediated inhibition of HSC activation (*SI Appendix*, Fig. S8*C*). However, knockdown of both SMAD7 and VDR almost completely abrogated the effect of inhibition of IFN-γ on HSC activation (*SI Appendix*, Fig. S8*C*).

To further elucidate the roles of SMAD7 and VDR in IFN-γ–mediated inhibition of HSC activation, we observed the phosphorylation of SMAD2/3 and recruitment of VDR to the *Col1α1* promotor in HSCs after IFN-γ stimulation in the presence or absence of *SMAD7* and *VDR* siRNA. We found that IFN-γ induction reduced the phosphorylation of SMAD2/3, which was rescued in the presence of *SMAD7* siRNA, but not *VDR* siRNA (*SI Appendix*, Fig. S8*D*). The recruitment of VDR to the *Col1α1* promotor dramatically increased after IFN-γ stimulation, but this was rescued in the presence of *VDR* siRNA, but not *SMAD7* siRNA (*SI Appendix*, Fig. S8*E*). Taken together, these data indicate that IFN-γ blocks the activation of HSCs through induction of not only SMAD7, but also VDR via inhibition of *miR-351*.

Activation of VDR Signaling by Calcipotriol Attenuated Schistosomiasis-Related Hepatic Fibrosis. To investigate whether VDR signaling is involved in the progression of hepatic fibrosis induced by schistosome infection, mice were exposed to a mild dose of parasites and treated with calcipotriol, a low-calcemic analog of $1,25(OH)_2D_3$

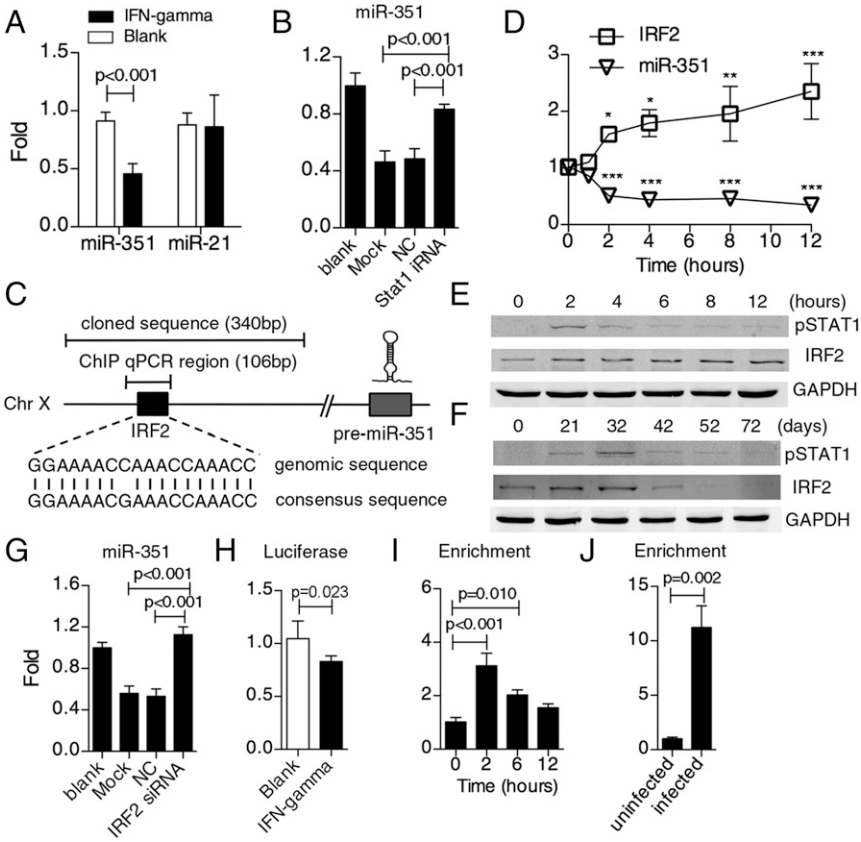

Fig. 3. IRF2 binds the promotor of the *pre–miR-351* to inhibit its transcription. (*A*) Expression of *miR-351* and *miR-21* in primary HSCs after IFN-γ stimulation ($n = 4$). (*B*) Expression of *miR-351* in primary HSCs after IFN-γ stimulation combined with knocking down *STAT1* using siRNA ($n = 4$). (*C*) Schematic diagram of the *pre–miR-351* genomic locus on the murine chromosome X. Predicted binding sites of IRF2 are shown as a black box. (*D*) Expression of *IRF2* and *miR-351* in primary HSCs after IFN-γ stimulation was detected by qPCR ($n = 4$). $^*P < 0.05$, $^{**}P < 0.001$, $^{***}P < 0.001$, compared with samples from 0 h. (*E*) Phosphorylation of STAT1 and expression of IRF2 in primary HSCs after IFN-γ stimulation was detected by Western blot. (*F*) Phosphorylation of STAT1 and expression of IRF2 in primary HSCs during infection was detected by Western blot. (*G*) Expression of *miR-351* in primary HSCs after IFN-γ stimulation combined with knocking down *IRF2* using siRNAs ($n = 4$). (*H*) The genomic region indicated by the bar above the *pre–miR-351* locus (*C*) was analyzed in a promoter luciferase reporter assay ($n = 6$). (*I* and *J*) ChIP-qPCR analysis of *pre–miR-351* promoter occupancy of IRF2 in primary HSCs after IFN-γ stimulation in vitro ($n = 3$) (*I*) or after 32 d of infection in vivo ($n = 3$) (*J*). Data are expressed as the mean ± SD of three independent experiments.

that activates VDR signaling (9). By 8 wk, calcipotriol-treated infected mice displayed a significant reduction in fibrosis compared with controls, as demonstrated by quantifications of hepatic hydroxyproline content, Masson's trichrome staining, and histological fibrotic scoring (Fig. 4 *A*, *B*, and *D*). These mice also had a marked reduction in the size of hepatic granulomas as determined by H&E staining (Fig. 4 *C* and *D*). Expression of key fibrotic marker genes, such as *Col1α1*, *Col3α1*, and *α-SMA*, were also significantly decreased by calcipotriol (Fig. 4 *E* and *F*). *CYP24A1* expression, a marker for activation of VDR signaling, was significantly elevated after calcipotriol treatment. However, the expression levels of *IL-13*, *TGF-β1*, and *IL-10* mRNA were similar for all groups of infected mice (Fig. 4*H*), and the livers showed no significant changes in parasite and egg burden (Fig. 4*I*). These data indicate that VDR signaling plays an important role in schistosomiasis-related hepatic fibrogenesis.

Discussion

Although many distinct signaling pathways contribute to the development of progressive fibrotic diseases, the TGF-β/SMAD pathway is considered one of the most potent profibrotic pathways in various organs. Blocking this pathway is a promising strategy for treating fibrosis (10). VDR is a recently identified antagonist of the TGF-β/SMAD pathway, and it is reported that down-regulation of VDR signaling plays a crucial role in the development of fibrosis in many organs, such as the liver (9), lung (21), kidney (22, 23), and heart (24). In this study, our data indicated that down-regulation of VDR signaling is crucial for the progression of hepatic fibrosis induced by schistosome infection, as significant reductions in hepatic fibrosis were observed upon up-regulation of VDR in the liver by rAAV8-mediated inhibition of *miR-351* or activation of VDR signaling in the liver by treatment with calcipotriol. Importantly, unlike other types of hepatic fibrosis, schistosome infection-induced hepatic fibrosis is believed to be IL-13 dependent, instead of TGF-β dependent (25). Therefore, our study suggests that VDR signaling is also involved in the progression of IL-13–dependent hepatic fibrosis. This is probably due to IL-13 activating the SMAD pathway to promote the activation of HSCs, which has been shown by several studies from our group and others (13, 26). Furthermore, our study revealed that VDR is regulated by *miR-351*, as up-regulation of *miR-351* leads to decreased VDR expression in HSCs, promoting hepatic fibrosis after infection. VDR was also reported to be targeted by other miRNAs (27–31), such as *miR-125b* and *miR-27b*. Notably, *miR-351* and *miR-125b* are from a miRNA family that shares the same seed sequence, indicating that this miRNA family plays a crucial role in the regulation of VDR expression.

Numerous studies have suggested that IFN-γ has antifibrotic activity (32). Mechanistically, IFN-γ is believed to inhibit fibrosis through blocking the profibrotic activity of SMAD signaling by inducing the expression of SMAD7, an antagonistic SMAD that interferes with the activation of SMAD2 and SMAD3 by preventing their receptor interaction and phosphorylation (18–20). In this study, we uncovered a mechanism for the antifibrotic effects of IFN-γ. Specifically, IFN-γ induces the expression of VDR, which antagonizes SMAD signaling, through inhibition of *miR-351*. VDR is an antagonist of SMAD signaling, which antagonizes SMAD residency on chromatin to suppress SMAD-dependent gene expression (9). Thus, IFN-γ simultaneously induces the expression of SMAD7 and VDR, which have synergic effects that block SMAD signaling. Importantly, this study also uncovers the mechanism by which IFN-γ induces the expression of VDR through inhibiting the expression of *miR-351*. IFN-γ acts through a pathway dependent on the transcription factor STAT1 to induce expression of IRF2, which binds the promotor of *pre–miR-351* to inhibit its transcription.

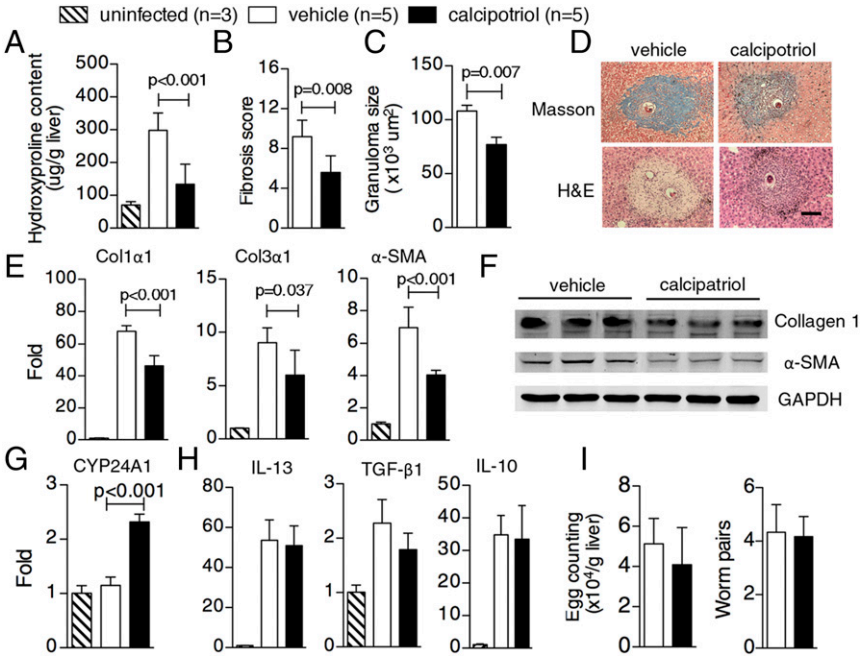

Fig. 4. Calcipotriol treatment attenuates schistosome-induced hepatic fibrosis in mice. Mice were infected percutaneously with 16 *S. japonicum* cercariae at day 0 or remained uninfected. Calcipotriol (20 mg/kg) was administered via oral gavage five times every week after infection, and liver samples were collected at day 56 postinfection. (*A*) Hydroxyproline content in the liver. Striped bars, uninfected mice ($n = 3$); white bars, mice receiving vehicle ($n = 5$); and black bars, mice receiving calcipotriol ($n = 5$). (*B*) Fibrosis scores measured from Masson's trichrome staining of liver sections. (*C*) Granuloma size measured from H&E staining of liver sections. (*D*) Masson's trichrome staining and H&E staining of liver sections. (Scale bar, 200 μm.) (*E*) qPCR analysis of levels of *Col1α1*, *Col3α1*, and *α-SMA* mRNA in the liver. (*F*) Western blot analysis of levels of collagen 1 and α-SMA in the liver. (*G*) qPCR analysis of levels of *CYP24a1* mRNA in the liver. (*H*) qPCR analysis of levels of *IL-13* and *TGF-β1* mRNA in the liver. (*I*) The number of eggs trapped in the livers and parasite pairs living in the hosts. Data are expressed as the mean ± SD of two independent experiments.

Here, we proposed a schematic diagram showing the molecular mechanism underpinning the regulation of schistosomiasis-induced hepatic fibrosis by miR-351 (*SI Appendix*, Fig. S9): at the early stages of *Schistosoma* infection, the schistosomula and adult worms induce expression of IFN-γ. The elevated IFN-γ up-regulates expression of both IRF2 and SMAD7 through activation of STAT1. The resulting SMAD7 inhibits SMAD2/3 by blocking their phosphorylation in the cytoplasm, while the IRF2 binds the promoter of *pre–miR-351* to down-regulate the expression of *miR-351*. Elevated VDR, resulting from *miR-351* reduction, inhibits SMAD2/3 by blocking their binding to promotor of fibrosis-related genes in the nucleus. However, at the later stages of the infection, when liver-trapped eggs are present, the host-produced cytokines switches from a Th1 to Th2 type, and thus IFN-γ declines. The elevated *miR-351* induces activation of HSCs and promotes hepatic fibrosis through production of *Col1α1*, *Col3α1*, and *α-SMA* by targeting VDR. Regarding the question of how *miR-351* expression is increased at the later stages of infection once levels of IFN-γ drop in infected mice, we have shown that the prototypical type 2 cytokines, including IL-4, IL-13, and TGF-β1 had no effect on *miR-351* expression in HSCs (*SI Appendix*, Fig. S10*A*). We also showed that neither IL-13 nor TGF-β1 relieved the inhibitory effect of IFN-γ on the expression of *miR-351* (*SI Appendix*, Fig. S10*B*). We speculate that the increase of *miR-351* expression could be due to the decline of IRF2 expression at the later stage of infection as shown in Fig. 3*F*. The reduced IRF2 can relieve the inhibition of transcription of *pre–miR-351*, leading to an increase of miR-351 expression. Of course, we do not exclude the possibility that other signaling pathways or factors could be involved in the regulation of *miR-351* expression.

Fibrosis is the final pathological outcome for many chronic inflammatory diseases. It affects nearly every organ in the body and can lead to permanent scarring, organ malfunction, and ultimately death. It is reported that fibrotic diseases account for more than 45% of deaths in the developed world. However, until now, there are no approved antifibrotic therapies (32). Aberrant miRNA expression is a common hallmark of many human diseases, including fibrotic diseases. Numerous studies have demonstrated that targeting dysregulated miRNAs using gene delivery systems is a promising therapeutic approach for treating fibrotic diseases (12). However, efficient, long-term, and safe delivery of miRNAs or their inhibitors to a diseased organ is always the bottleneck of a miRNA-based strategy (33). In this study, we chose the rAAV8 vector to deliver a miRNA sponge into a fibrotic liver. This strategy was based on its liver tropism and safety and efficacy in a variety of preclinical and clinical studies (34). Importantly, we demonstrated that rAAV8-mediated inhibition of *miR-351* protects hosts from the lethal effects of schistosome infection through attenuation of hepatic fibrosis. Up-regulation of *miR-351* following infection decreases VDR levels, which contributes to fibrosis by activating SMAD signaling. In addition, VDR is reported to reduce the development of fibrosis in many organs. Therefore, rAAV8-mediated inhibition of *miR-351* might provide a useful strategy for treating these fibrotic diseases.

Methods

Six-week-old male BALB/c mice were purchased from the experimental animal center of the Second Military Medical University. The mice were acclimatized to the laboratory environment for at least 7 d at a constant temperature (23 ± 2 °C) before being infected. For infections, mice were exposed to 16 or 30 *S. japonicum* cercariae percutaneously. Cercariae were obtained from the National Institute of Parasitic Disease at the Chinese Center for Disease Control and Prevention. All protocols performed on animals for this study obeyed the Guide for the Care and Use of Laboratory Animals of the National Institutes of Health, and they were approved by the Animal Ethics Committee of the Second Military Medical University [laboratory animal usage number FYXK (Shanghai) 2014–0003].

A detailed description of methodologies used in this study can be found in *SI Appendix*.

ACKNOWLEDGMENTS. We thank the staff of the National Institute of Parasitic Disease, Chinese Center for Disease Control and Prevention for their help with parasite infections. This study was supported by the National Natural Science Foundation of China (81501767 and 81430051).

1. Colley DG, Bustinduy AL, Secor WE, King CH (2014) Human schistosomiasis. *Lancet* 383:2253–2264.
2. Weerakoon KG, Gobert GN, Cai P, McManus DP (2015) Advances in the diagnosis of human schistosomiasis. *Clin Microbiol Rev* 28:939–967.
3. Pearce EJ, MacDonald AS (2002) The immunobiology of schistosomiasis. *Nat Rev Immunol* 2:499–511.
4. Wilson MS, et al. (2007) Immunopathology of schistosomiasis. *Immunol Cell Biol* 85: 148–154.
5. Friedman SL (2008) Hepatic stellate cells: Protean, multifunctional, and enigmatic cells of the liver. *Physiol Rev* 88:125–172.
6. Bartley PB, et al. (2006) A contributory role for activated hepatic stellate cells in the dynamics of *Schistosoma japonicum* egg-induced fibrosis. *Int J Parasitol* 36:993–1001.
7. Friedman SL (2008) Mechanisms of hepatic fibrogenesis. *Gastroenterology* 134: 1655–1669.
8. Massagué J, Seoane J, Wotton D (2005) Smad transcription factors. *Genes Dev* 19: 2783–2810.
9. Ding N, et al. (2013) A vitamin D receptor/SMAD genomic circuit gates hepatic fibrotic response. *Cell* 153:601–613.
10. Gressner AM, Weiskirchen R (2006) Modern pathogenetic concepts of liver fibrosis suggest stellate cells and TGF-beta as major players and therapeutic targets. *J Cell Mol Med* 10:76–99.
11. Esteller M (2011) Non-coding RNAs in human disease. *Nat Rev Genet* 12:861–874.
12. Jiang X, Tsitsiou E, Herrick SE, Lindsay MA (2010) MicroRNAs and the regulation of fibrosis. *FEBS J* 277:2015–2021.
13. He X, et al. (2015) Recombinant adeno-associated virus-mediated inhibition of microRNA-21 protects mice against the lethal schistosome infection by repressing both IL-13 and transforming growth factor beta 1 pathways. *Hepatology* 61:2008–2017.
14. Xie T, et al. (2011) Comprehensive microRNA analysis in bleomycin-induced pulmonary fibrosis identifies multiple sites of molecular regulation. *Physiol Genomics* 43:479–487.
15. Wahl SM, et al. (1997) Cytokine regulation of schistosome-induced granuloma and fibrosis. *Kidney Int* 51:1370–1375.
16. Billiau A, Matthys P (2009) Interferon-gamma: A historical perspective. *Cytokine Growth Factor Rev* 20:97–113.
17. Tanaka N, Kawakami T, Taniguchi T (1993) Recognition DNA sequences of interferon regulatory factor 1 (IRF-1) and IRF-2, regulators of cell growth and the interferon system. *Mol Cell Biol* 13:4531–4538.
18. Jeong WI, Park O, Gao B (2008) Abrogation of the antifibrotic effects of natural killer cells/interferon-gamma contributes to alcohol acceleration of liver fibrosis. *Gastroenterology* 134:248–258.
19. Weng H, Mertens PR, Gressner AM, Dooley S (2007) IFN-gamma abrogates profibrogenic TGF-beta signaling in liver by targeting expression of inhibitory and receptor Smads. *J Hepatol* 46:295–303.
20. Nakao A, Okumura K, Ogawa H (2002) Smad7: A new key player in TGF-beta-associated disease. *Trends Mol Med* 8:361–363.
21. Ramirez AM, et al. (2010) Vitamin D inhibition of pro-fibrotic effects of transforming growth factor beta1 in lung fibroblasts and epithelial cells. *J Steroid Biochem Mol Biol* 118:142–150.
22. Gonçalves JG, et al. (2014) Vitamin D deficiency aggravates chronic kidney disease progression after ischemic acute kidney injury. *PLoS One* 9:e107228.
23. Ito I, et al. (2013) A nonclassical vitamin D receptor pathway suppresses renal fibrosis. *J Clin Invest* 123:4579–4594.
24. Bae S, et al. (2013) Vitamin D signaling pathway plays an important role in the development of heart failure after myocardial infarction. *J Appl Physiol (1985)* 114: 979–987.
25. Kaviratne M, et al. (2004) IL-13 activates a mechanism of tissue fibrosis that is completely TGF-beta independent. *J Immunol* 173:4020–4029.
26. Liu Y, et al. (2011) IL-13 induces connective tissue growth factor in rat hepatic stellate cells via TGF-β-independent Smad signaling. *J Immunol* 187:2814–2823.
27. Li F, Zhang A, Shi Y, Ma Y, Du Y (2015) 1α,25-Dihydroxyvitamin D3 prevents the differentiation of human lung fibroblasts via microRNA-27b targeting the vitamin D receptor. *Int J Mol Med* 36:967–974.
28. Mohri T, Nakajima M, Takagi S, Komagata S, Yokoi T (2009) MicroRNA regulates human vitamin D receptor. *Int J Cancer* 125:1328–1333.
29. Chen Y, et al. (2014) MicroRNA-346 mediates tumor necrosis factor α-induced downregulation of gut epithelial vitamin D receptor in inflammatory bowel diseases. *Inflamm Bowel Dis* 20:1910–1918.
30. Essa S, et al. (2010) VDR microRNA expression and epigenetic silencing of vitamin D signaling in melanoma cells. *J Steroid Biochem Mol Biol* 121:110–113.
31. Lisse TS, Adams JS, Hewison M (2013) Vitamin D and microRNAs in bone. *Crit Rev Eukaryot Gene Expr* 23:195–214.
32. Wynn TA, Ramalingam TR (2012) Mechanisms of fibrosis: Therapeutic translation for fibrotic disease. *Nat Med* 18:1028–1040.
33. Pai SI, et al. (2006) Prospects of RNA interference therapy for cancer. *Gene Ther* 13: 464–477.
34. Grieger JC, Samulski RJ (2005) Adeno-associated virus as a gene therapy vector: Vector development, production and clinical applications. *Adv Biochem Eng Biotechnol* 99: 119–145.